ELSEVIER

Bone 41 (2007) 247–255

BONE

www.elsevier.com/locate/bone

BMP-silk composite matrices heal critically sized femoral defects

C. Kirker-Head [a], V. Karageorgiou [b], S. Hofmann [b,c], R. Fajardo [d], O. Betz [e], H.P. Merkle [c], M. Hilbe [f], B. von Rechenberg [g], J. McCool [a], L. Abrahamsen [a], A. Nazarian [d], E. Cory [d], M. Curtis [b], D. Kaplan [b,*], L. Meinel [b,c,h]

[a] *Tufts Cummings School of Veterinary Medicine, North Grafton, MA, USA*
[b] *Departments of Biomedical Engineering & Chemical and Biological Engineering, Tufts University, Medford, MA, USA*
[c] *Department of Chemistry and Applied Biosciences, ETH Zurich, Switzerland*
[d] *Orthopaedic Biomechanics Laboratory, Beth Israel Deaconess Medical Center, Harvard Medical School, Boston, MA, USA*
[e] *Center for Molecular Orthopaedics, Brigham and Women's Hospital, Harvard Medical School, Boston, MA, USA*
[f] *Institute of Veterinary Pathology, Vetsuisse Faculty, University of Zurich, Zurich, Switzerland*
[g] *Musculoskeletal Research Unit, Faculty of Veterinary Medicine, University of Zurich, Zurich, Switzerland*
[h] *Division of Health Sciences and Technology, Massachusetts Institute of Technology, Cambridge, MA, USA*

Received 10 July 2006; revised 9 April 2007; accepted 14 April 2007
Available online 27 April 2007

Abstract

Clinical drawbacks of bone grafting prompt the search for alternative bone augmentation technologies such as use of growth and differentiation factors, gene therapy, and cell therapy. Osteopromotive matrices are frequently employed for the local delivery and controlled release of these augmentation agents. Some matrices also provide an osteoconductive scaffold to support new bone growth. In this study, silkworm-derived silk fibroin was evaluated as an osteoconductive matrix for healing critical sized mid-femoral segmental defects in nude rats. Four treatment groups were assessed over eight weeks: silk scaffolds (SS) with recombinant human BMP-2 (rhBMP-2) and human mesenchymal stem cells (HMSC) that had been pre-differentiated along an osteoblastic lineage ex vivo (Group I; pdHMSC/rhBMP-2/SS); SS with rhBMP-2 and undifferentiated HMSCs (Group II; udHMSC/rhBMP-2/SS); SS and rhBMP-2 alone (Group III; rhBMP-2/SS); and empty defects (Group IV). Bi-weekly radiographs revealed a progressive and similar increase in Group I–III mean defect mineralization through post-operative week (POW) 8. Radiographs, dual energy x-ray absorptiometry, and micro-computed tomography confirmed that Groups I–III exhibited similar substantial and significantly ($p<0.05$) greater defect mineralization at POW 8 than the unfilled Group IV defects which remained void of bone. No significant differences in Groups I–III defect healing at POW 8 were apparent using these same assays or mechanical testing. Histology at POW 8 revealed moderately good bridging of the parent diaphyseal cortices with woven and lamellar bone bridging islands of silk matrix in Groups I and III. Group II defects possessed comparatively less new bone which was most abundant adjacent to the parent bone margins. Elsewhere the silk matrix was more often enveloped by poorly differentiated loose fibrous connective tissue. Group IV defects showed minimal new bone formation. None of the treatment groups attained the mean mineralization or the mean biomechanical strength of identical defects implanted with SS and pdHMSCs alone in a previous study. However, addition of rhBMP-2 to SS prompted more bone than was previously generated using udHMSC/SS or SS alone. These data imply the clinical potential of silk scaffolds and rhBMP-2 as composite osteopromotive implants when used alone or with select stem cell populations. Additional studies in larger species are now warranted.

Keywords: Bone healing; Silk implant; Bone morphogenetic protein; Human mesenchymal stem cells; Tissue engineering; Long bone defect

Introduction

Refinements in anesthetic and surgical techniques, implant design and application and peri-operative management have significantly improved the treatment of complex fractures and other skeletal defects caused by trauma, disease, developmental

* Corresponding author. Fax: +1 617 627 3251.
E-mail address: david.kaplan@tufts.edu (D. Kaplan).

8756-3282/$ - see front matter © 2007 Elsevier Inc. All rights reserved.
doi:10.1016/j.bone.2007.04.186

deformity and tumor resection. Nonetheless, an unfavorable wound environment, sub-optimal surgical technique or biomechanical instability can all lead to delayed or non-union. Under these circumstances, bone grafts have been the principal means of augmenting or accelerating bone regeneration, and as many as 1.5 million per year are carried out in the United States [1].

Unfortunately, significant drawbacks are associated with the use of this approach such as: the need for additional anesthetic time or personnel for graft harvesting; an insufficient quantity of graft, limited access to donor sites, loss of osteogenic cells, donor site pain or hemorrhage, and predisposition of the donor bone to failure. Vascularized autografts are technically demanding and allografts and xenografts carry the hazards of immune-mediated rejection, graft sequestration and transmission of infection between donor and host. Also, bone banks are costly to maintain [2].

Accordingly, investigators have been pursuing alternative bone augmentation technologies and several novel approaches to bone regeneration now hold promise for clinical application, among them the use of bone growth and differentiation factors [3], gene therapy [4] and cell therapy [5]. In each instance, osteopromotive matrices are frequently employed for the local delivery and controlled release of the augmentation agents [2]. Some also provide an osteoconductive physical scaffold for neo-vascularization and neo-osteogenesis [2].

A wide range of organic and inorganic materials have been tested as osteoconductive matrices both in vitro and in vivo [2,3], among them *Bombyx mori* silkworm silk fibroin [6–8]. Our ability to genetically, physically and chemically manipulate *B. mori* silk allows us to generate silk matrices that are biocompatible, mechanically strong, stable at physiological temperatures and predictably degradable [6,9]. Studies imply their osteoconductive potential, particularly when combined with a responsive population of stem cells and/or osteoinductive cytokines: when critical size cranial defects in mice were implanted with silk scaffolds (SS) and a population of human mesenchymal stem cells (HMSCs) pre-differentiated along an osteoblastic lineage (pdHMSC/SS), substantial bone regeneration occurred [7]. When a similar pdHMSC/SS was implanted in critical size weight-bearing femoral defects in rats, bone regeneration was correspondingly prominent and the defects progressed towards healing [10]. In both defect models, however, bone regeneration was less substantial when the silk matrix was implanted alone (SS) or with undifferentiated HMSCs (udHMSC/SS) [10,7]. Using a murine cranial defect model, we subsequently demonstrated that these latter limited osteogenic responses could be effectively enhanced by pre-loading the SS or udHMSC/SS implants immediately prior to implantation with a supraphysiological dose of recombinant human BMP-2 (rhBMP-2), a potent osteoinductive cytokine [11].

In this study we used a rat critical size femoral defect model to determine if a single application of a supraphysiological quantity of rhBMP-2 could enhance the osteogenic response to SS implanted alone or with udHMSCs or pdHMSCs. Three treatment groups and one control group were assessed: (i) silk, rhBMP-2 and pre-differentiated HMSCs (pdHMSC/rhBMP-2/SS); (ii) silk, rhBMP-2 and undifferentiated HMSCs (udHMSC/rhBMP-2/SS); (iii) silk and rhBMP-2 alone (rhBMP-2/SS); and a no implant control. A series of radiographic, absorptiometric, micro-computed tomographic, biomechanical, and histological analyses were employed to generate the data.

Materials and methods

Experimental design

Critical size femoral defects were surgically created in the right hind limb of 24 rats. At the time of surgery (post-operative week [POW] 0) rats were randomly assigned to one of four defect treatment groups (Table 1). Group I ($n=6$) received rhBMP-2 loaded silk scaffolds which had been seeded with undifferentiated HMSCs and then incubated in osteogenic medium for 4 weeks prior to implantation (pdHMSC/rhBMP-2/SS); Group II ($n=6$) received rhBMP-2 loaded silk scaffolds seeded with undifferentiated HMSCs 1 day prior to implantation (udHMSC/rhBMP-2/SS); Group III ($n=6$) received rhBMP-2 loaded silk scaffolds devoid of cells (rhBMP-2/SS); and in Group IV ($n=6$), defects were left empty (control). Radiographs of the operated limb were completed at post-operative weeks (POW) 0, 2, 4, 6, and 8. Animals were sacrificed at POW 8 and femora underwent dual energy x-ray absorptiometry (DEXA) analyses. The operated femora were then frozen for biomechanical testing and micro-computed tomography (μCT) or placed in 4 °C 4% paraformaldehyde for histological and immunohistochemical evaluation.

Materials

Silkworm cocoons were kindly supplied by M. Tsukada, Institute of Sericulture, Tsukuba, Japan, and Marion Goldsmith, University of Rhode Island. Recombinant human BMP-2 was kindly supplied by Wyeth Biopharmaceuticals, Andover, MA. Dulbecco's Modified Eagle Medium (DMEM), RPMI 1640 medium, Fetal Bovine Serum (FBS), basic fibroblast growth factor (bFGF), penicillin and streptomycin (Pen–Strep), Fungizone, trypsin and nonessential amino acids (NEAA, consisting of 8.9 mg/L L-alanine, 13.21 mg/L L-asparagine, 13.3 mg/L L-aspartic acid, 14.7 mg/L L-glutamic acid, 7.5 mg/L glycine, 11.5 mg/L L-proline, 10.5 mg/L L-serine) were from Gibco (Carlsbad, CA). Histopaque-1077, Ascorbic acid-2-phosphate and dexamethasone were from Sigma (St. Louis, MO). All other substances were obtained from Sigma.

Scaffold preparation and characterization

Extraction and purification of silk fibroin from *B. mori* silkworm cocoons have been previously described [12], as has silk scaffold preparation [11].

Table 1
Description of the four treatment groups and their rhBMP-2 contents

Group	Abbreviation	Description	SS rhBMP-2 content
I	pdHMSC/rhBMP-2/SS	Human mesenchymal stem cells seeded on recombinant human bone morphogenetic protein-2 loaded silk scaffolds and differentiated under osteogenic conditions for 4 weeks in spinner flasks prior to implantation	2.5 (2.4±0.14 [SD]) μg rhBMP-2
II	udHMSC/rhBMP-2/SS	Undifferentiated human mesenchymal stem cells seeded on recombinant human bone morphogenetic protein-2 loaded silk scaffolds 1 day prior to implantation	2.5 (2.4±0.14 [SD]) μg rhBMP-2
III	rhBMP-2/SS	Recombinant human bone morphogenetic protein-2 loaded silk scaffolds without cells	2.5 (2.4±0.14 [SD]) μg rhBMP-2
IV	Control	No implant — empty defects	–

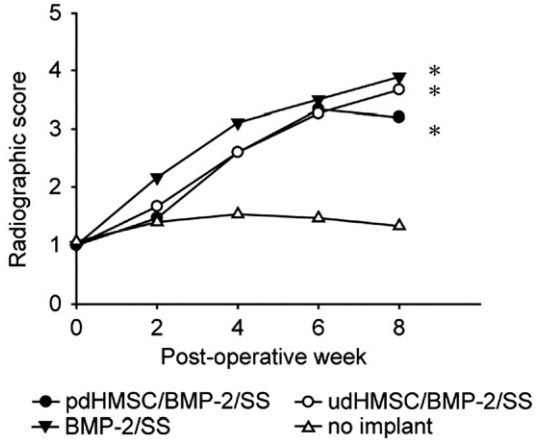

Fig. 1. Radiographic assessment of defect mineralization. Radiographs were completed immediately post-implantation (POW 0) and then every second week (POW 2, 4, 6, and 8). Defect mineralization was semi-quantitatively graded using the following standardized scale: 1. trace radiodense material in defect; 2. flocculent radiodensity and incomplete bridging of the defect; 3. bridging of the defect at 1+ location; 4. bridging of the defect at *cis* and *trans* cortices, parent cortex visible; 5. one cortex obscured by new bone; 6. bridging of the defect by uniform new bone, cut ends of cortex not seen [14]. *Significantly ($p < 0.05$) greater than Group IV data.

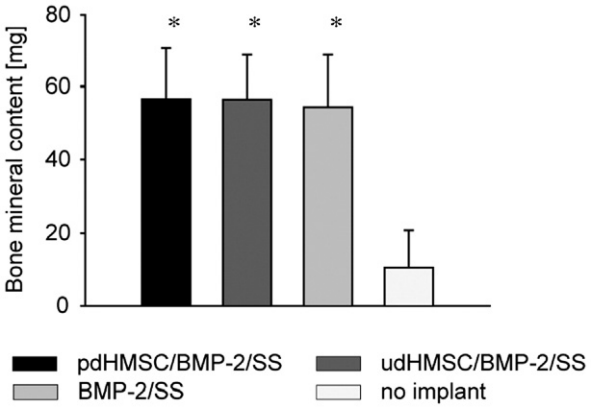

Fig. 2. Regenerate bone mineral content (BMC) acquired by DEXA analysis of the operated limb immediately post-sacrifice (POW 8). Error bars reflect 1 standard deviation. *Significantly ($p < 0.05$) greater than Group IV data.

Briefly, following purification, the silk was lyophilized and redissolved in 1,1,1,3,3,3-hexafluoro-2-propanol (HFIP) to obtain a 17% (w/v) solution. Granular NaCl was added to the silk/HFIP solution at a ratio of 20:1 (NaCl/silk). HFIP was allowed to evaporate for 3 days and NaCl/silk blocks were immersed in 90% (v/v) methanol for 30 min to induce a protein conformational transition to an insoluble β-sheet structure [10]. Blocks were removed, dried and NaCl was extracted by incubation in water for 2 days. Disk shaped scaffolds (8 mm diameter, 2 mm thick) were created using a dermal punch and autoclaved at 121 °C for 15 min. Recombinant human BMP-2, supplied in a formulation buffer, was dialyzed against 0.5 M arginine, 5 mM glutamic acid, at a pH 3.8 for 1 day, 0.5 M arginine and Dulbecco's Phosphate Buffered Saline (D-PBS) for another day and D-PBS for 2 days. The protein solution was sterilized with 0.22 μm syringe filters (Millipore, Billerica, MA). Scaffolds were transferred into 10 ml syringes (Becton Dickinson, Franklin Lakes, NJ) and contacted with 1.5 ml of 0.05 mg/ml rhBMP-2 in D-PBS solution for 6 h. The procedure was carried out aseptically.

Cell isolation, expansion and characterization

Cell preparation has been previously described [11,10]. Briefly, HMSCs were isolated by density gradient centrifugation (800×*g*; 30 min) of whole bone marrow (Clonetics, Santa Rosa, CA) diluted (1:10 v/v) in *isolation medium* (RPMI 1640 supplemented with 5% FBS) over a poly-sucrose gradient (1.077 g/cm^3, Histopaque, Sigma, St. Louis, MO). The cell layer was removed, washed in isolation medium, pelleted at 300×*g* and contaminating red blood cells were eliminated using Pure-Gene RBC Lysis solution (Gentra Systems Inc, Minneapolis, MN). Cells were then suspended in *expansion medium* (DMEM, 10% FBS, Pen–Strep, Fungizone, NEAA and 1 ng/ml bFGF) and seeded in flasks at a density of 5×10^4 cells/cm^2. Adherent cells were allowed to reach approximately 80% confluence, requiring 12–17 days for the first passage before being replated.

For preparation of the Group I implants (pdHMSC/rhBMP-2/SS), second passage HMSCs were suspended in liquid BD Matrigel Basement Membrane Matrix (BD Biosciences, San Jose, CA) before being seeded onto silk scaffolds loaded with 2.5 (2.4±0.14 [SD]) μg rhBMP-2 as quantified with I^{125}-BMP-2 [11]. The composite implants were then placed in spinner flasks as previously described [11,7] for 4 weeks prior to surgical implantation. The flasks were filled with *osteogenic medium* (DMEM supplemented with 10% FBS, Pen–Strep and Fungizone supplemented with 50 μg/ml ascorbic acid-2-phosphate, 10 nM dexamethasone, 7 mM β-glycerolphosphate) which, in combination with the rhBMP-2, prompted pre-differentiation of the HMSCs along an osteoblastic lineage (pdHMSCs). Flasks were placed unsealed in a humidified incubator (37 °C, 5% CO_2) which permitted gas exchange and stirred with a magnetic bar. Medium (but not rhBMP-2) was replaced at a rate of 50% every 2–3 days for the 4 weeks of cultivation [11]. Group II implants (udHMSC/rhBMP-2/SS) were prepared by seeding second passage HMSCs onto silk scaffolds loaded with 2.5 (2.4±0.14 [SD]) μg rhBMP-2 on the day immediately prior to surgical implantation. Group III implants were silk scaffolds loaded with 2.5 (2.4±0.14 [SD]) μg rhBMP-2 [11] but no cells.

Operative procedure

A critical size, femoral defect rat model was used in this study [13]. All procedures were approved by the operative institution's Animal Care and Use Committee. Briefly, adult, male athymic T-cell deficient RH-rnu rats weighing 325–400 g were placed under general anesthesia and maintained using inhalant isofluorane and oxygen. The rats were positioned in lateral recumbency and the

Table 2
Quantitative summary data for radiographic, densitometric, micro-CT, and biomechanical tests

Treatment	Radiography (scalar 1–6)	Densitometry (mg)	Micro-CT	Biomechanics	
			Bone volume/defect (mm^3)	Maximal load (N)	Maximal torque (Nm)
pdHMSC/rhBMP-2/SS	3.20±0.29^a	56.65±13.93^a	70.48±7.99^a	10.82±1.59	1.78±0.53
udHMSC/rhBMP-2/SS	3.67±0.82^a	56.46±12.26^a	63.49±24.29^a	7.53±1.41	0.87±0.29
rhBMP-2/SS	3.89±0.58^a	54.35±14.38^a	69.92±8.32^a	8.76±3.59	1.31±1.17
No implant	1.33±0.82^b	10.52±10.27^b	23.78±11.74^b	NM	NM
pdHMSC/SS [10]	NM	NM	207.41±13.94$^\infty$	11.73±1.42$^\infty$	2.08±0.50$^\infty$
udHMSC/SS [10]	NM	NM	46.78±0.92$^\infty$	8.03±1.00$^\infty$	0.98±0.24$^\infty$
SS [10]	NM	NM	63.65±2.09$^\infty$	5.15±0.22$^\infty$	0.40±0.03$^\infty$

Within column differences in superscript Arabic lettering denote the existence of statistically significant differences in numeric values. NM=not measured. ∞=not statistically analyzed against this study's data.

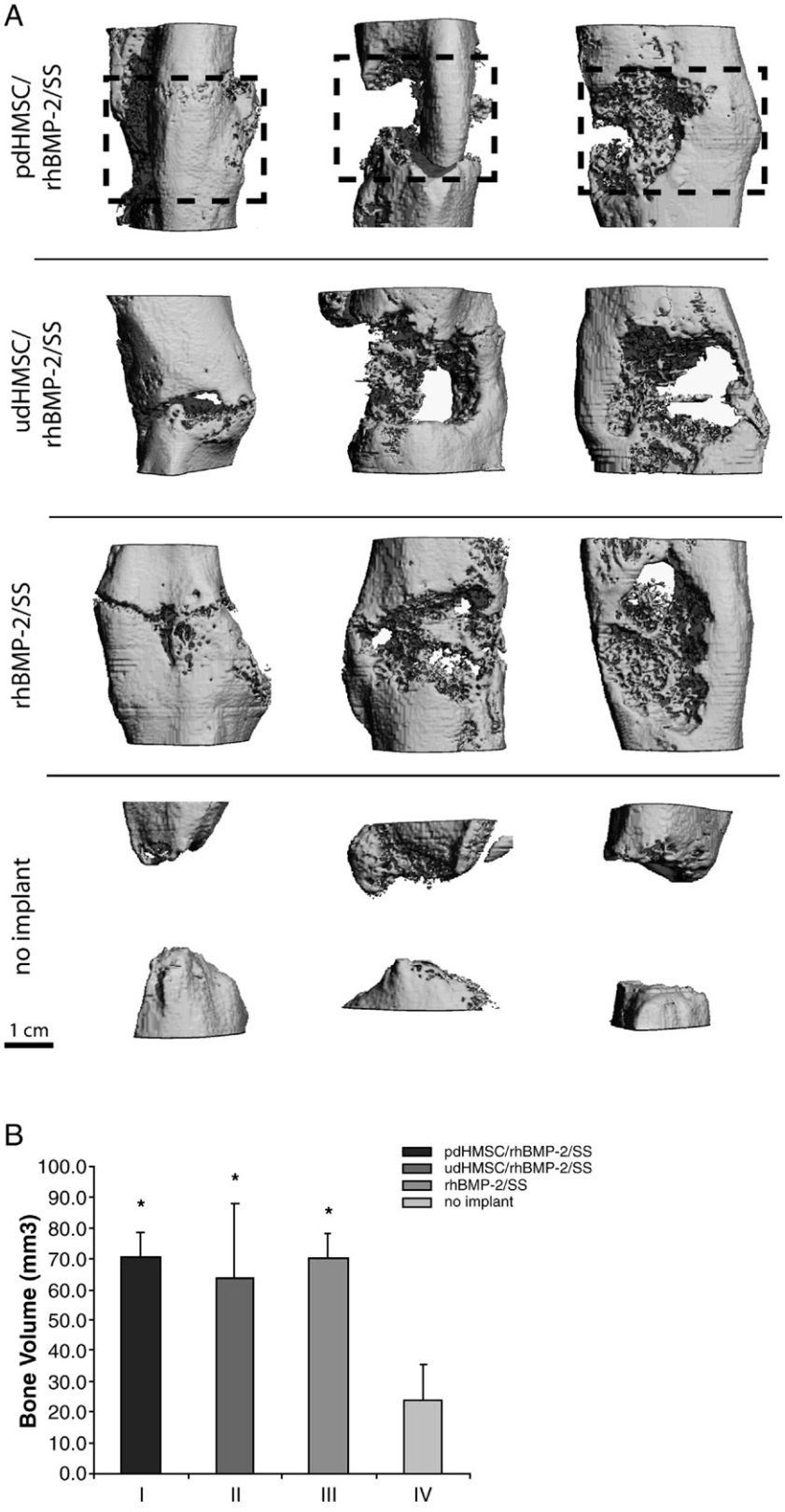

Fig. 3. (A) Micro-computed tomography from three representative rat critical size femoral defects for each treatment group 8 weeks after surgery. The dotted box approximately indicates the original defect zone. (B) Morphometric analysis (bone volume per defect, [mm^3]) of new bone formation from rat critical size femoral defects 8 weeks after surgery and treated with pdHMSC grown for 5 weeks on rhBMP-2 loaded silk scaffolds (group I), rhBMP-2 loaded silk scaffolds seeded with udHMSC (group II), unseeded rhBMP-2 loaded silk scaffolds (group III), and untreated (control) defects (group IV). Error bars reflect 1 standard deviation. *Significantly ($p < 0.05$) greater than Group IV data.

uppermost hindlimb was aseptically prepared for surgery. An approximately 25 mm long skin incision was created over the femur and underlying soft tissues were retracted to reveal the bone. One pair of 1.1-mm external diameter self tapping threaded pins were placed transcortically in a latero-medial plane in the proximal femur and a second pair were similarly placed in the distal femur, leaving the mid-diaphysis readily accessible. The pin tips extended 0.5 mm beyond the *trans* cortex. Four small stab incisions were made in the skin, allowing it to be re-seated over the pins and an external fixator bar was secured to all 4 pins with miniscrews. A high speed dental drill was used to carefully create a 5-mm long full thickness osteo-periosteal critical size defect in the mid-diaphysis which was subsequently filled with the test implant. Overlying soft tissues were then routinely closed.

Radiography

Standardized digital radiographs (Kodak Directview Version 5.2, Eastman Kodak, Rochester, NY) of the operated femurs were completed immediately post-implantation (POW 0) and then every second week (POW 2, 4, 6 and 8) for the duration of the study. Defect mineralization was semi-quantitatively graded by 2 radiologists blinded to the treatment groups, using a standardized scale (1. trace radiodense material in defect; 2. flocculent radiodensity and incomplete bridging of the defect; 3. bridging of the defect at 1+ location; 4. bridging of the defect at *cis* and *trans* cortices, parent cortex visible; 5. one cortex obscured by new bone; 6. bridging of the defect by uniform new bone, cut ends of cortex not seen) [14].

Dual energy x-ray absorptiometry

Immediately post-sacrifice (POW 8), a region of interest (ROI) corresponding to the 5-mm long bone defect (as created at the time of surgery) in the coronal plane and extending sufficiently far in the sagittal plane (i.e. perpendicular to the long axis of the femur) as to incorporate all regenerative bone underwent DEXA analysis (QDR 4500 Acclaim Elite, Hologic, Inc, MA). The standardized position of the transfixation pin holes relative to each other and the defect helped insure consistency in positioning the ROI. The generated data provided a means of quantifying regenerate bone mineral content (BMC) (g). A sub-region high resolution software algorithm was employed.

Micro-computed tomography (μCT)

As a means of assessing defect 3-D bone regeneration, operated femora were analyzed at POW 8 using a μCT40 imaging system (Scanco Medical, Bassersdorf, Switzerland). The fixator pins' positions relative to each other and the defect also insured consistency in locating the volume of interest (VOI). VOIs extended in the coronal plane between the transfixation pin holes adjacent to the defect and they extended sufficiently far outward in the sagittal plane as to include all regenerative bone. The following scan parameters were employed: 20 mm field of view, 55 kVp x-ray energy setting, 1024 reconstruction matrix, slice thickness 0.02 mm and a 250 millisecond integration time. Mineralized tissue was segmented from non-mineralized tissue using a global thresholding procedure with a value approximating 1.20 g/cm^3 (150 on μCT) (25% lower than 1.6 g/cm^3 which is the mineral density of healthy human compact bone) [15]. Bone volume per defect (BV; mm^3) was recorded as the measure of defect bone regeneration.

Mechanical testing

Both ends of the femora undergoing destructive mechanical testing were embedded in polymethylmethacrylate (PMMA). A novel torsional testing system was employed such that the axis of rotation of the torsional forces correlated with the geometric neutral axis of the cylindrical bone specimens. Torque was applied using a strain rate of 5 rad/min via a MTS200 screw axis load frame (MTS, Saint Paul, MN, USA). Data were collected with a LabVIEW (National Instruments, Austin, TX) acquisition system. Maximum load (N) and maximum torque (Nm) were measured for each specimen [10].

Histology and immunohistochemistry

Fixed and decalcified (12% EDTA, pH 7.0) femoral explants were dehydrated in graded ethanol solutions and xylene, embedded in paraffin and cut into 3-μm-thick sections. For a general overview, sections were stained with hematoxylin and eosin. Immunohistochemical studies were performed for bone sialoprotein (BSP) and collagen type I using a rabbit anti-bone sialoprotein II polyclonal antibody (Chemicon, Temecula, CA) and mouse anti-collagen type I monoclonal antibody (Sigma, St. Lois, MA) respectively, as previously described [10].

Statistical analysis

Quantitative data were evaluated for within or between group differences using a Student's *t*-test or an ANOVA where appropriate. Tomographic and biomechanical data were first tested for normality of distribution using a Kolmogorov–Smirnov analysis. ANOVA was followed by a *post hoc* assessment using the Tukey HSD method. All data were reported as means ±standard deviation (SD). Differences were considered significant when equal or less than $p=0.05$.

Results

Radiographic data

The semi-quantitative assessment of defect mineralization by 2 radiologists blinded to the treatments revealed a progressive and similar increase in mean defect mineralization from POW 0 through POW 8 for treatment Groups I (pdHMSC/rhBMP-2/SS), II (udHMSC/rhBMP-2/SS) and III (rhBMP-2/SS). At POW 8 these 3 groups' radiographic scores reflected bridging of the defect with new bone traversing between proximal and distal components of the *cis* and/or *trans* cortices. The parent bone cortices, however, were still well defined. Group I–III radiographic scores were significantly ($p<0.05$) greater than the unfilled control Group IV score at POW 8. Group IV defects reflected only the presence of trace mineralization (Fig. 1, Table 2). No other significant differences were observed between groups.

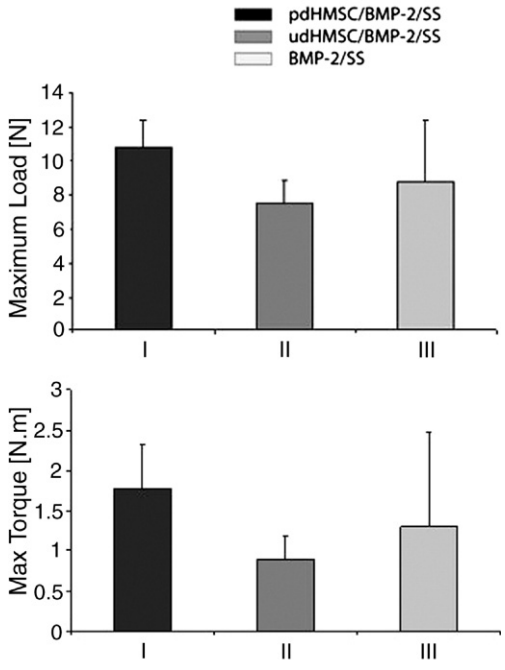

Fig. 4. Mechanical features of rat critical size femoral defects 8 weeks after implantation with pdHMSC/rhBMP-2/SS (Group I), udHMSC/rhBMP-2/SS (Group II) and SS alone (Group III). (A) Maximal load before failure and (B) maximal torque. Error bars reflect 1 standard deviation.

Dual energy x-ray absorptiometry (DEXA) data

Quantitative DEXA data confirmed that Groups I through III had similar and substantial mean defect bone mineral content at POW 8, which was significantly greater ($p < 0.05$) than that of the unfilled Group IV defect (Fig. 2; Table 2). No other significant differences were observed between groups.

Micro-CT data

At POW 8 the morphology of the formed bone within the defect was evaluated using μCT (Fig. 3A). Group IV defects showed little evidence of bone regeneration with the parent cortices at the defect margins remodeling to form a rounded cap characteristic of non-union. Groups I–III all demonstrated variable bridging of the defect. Group II defects more commonly exhibited large voids within the regenerated bone. In Groups I–III, bone was cortical like towards the periphery of the defect but more cancellous or sponge-like towards the defect's center. Several defects in Groups I–III had narrow cracks propagating across the full thickness of the regenerated bone. In all cases, new bone was limited to the immediate defect or a distance extending no more than approximately 2-mm beyond the parent diaphyseal diameter. Bone volume was

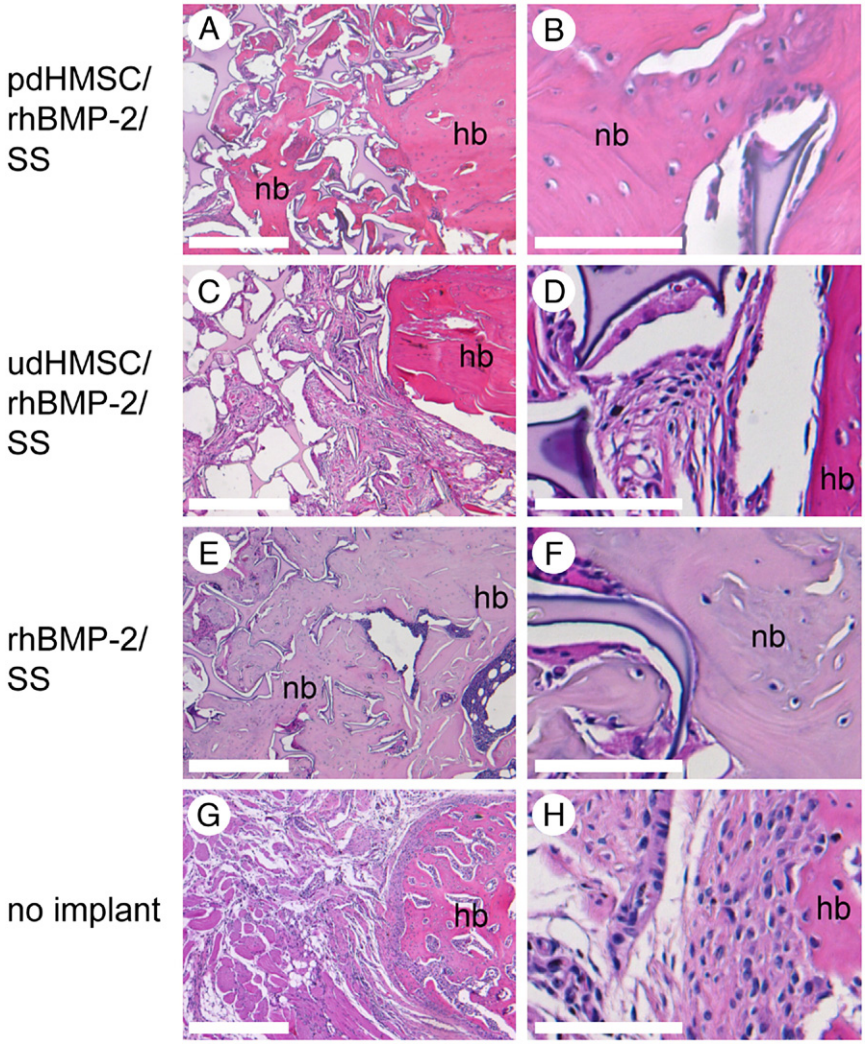

Fig. 5. Histological cross-sections taken from rat critical size femoral defects 8 weeks after surgery and stained with H&E; (A–B) pdHMSC on rhBMP-2 loaded silk scaffolds (Group I; pdHMSC/rhBMP-2/SS), (C–D) rhBMP-2 loaded silk scaffolds seeded with udHMSC (Group II; udHMSC/rhBMP-2/SS), (E–F) unseeded rhBMP-2 loaded silk scaffolds (Group III; rhBMP-2/SS), and (G–H) untreated (control) defects (Group IV; no implant). There is moderately good integration of the parent diaphyseal cortices with new bone in Groups I (A, B) and III (E, F). In both groups the defects were characterized by the presence of a continuum of woven and lamellar bone surrounding islands of silk matrix centrally with elements of cortical bone peripherally. The extent of trabecular bone in Group I defects (A, B) was moderately less than that noted in Group III (E, F) defects. Group II defects revealed comparatively less new bone formation than both Groups I and III and that present was principally found adjacent to the parent bone margins (C, D). The Group II silk matrix was often diffusely enveloped by poorly differentiated loose fibrous connective tissue (C, D). While few in number, there were moderately more cartilage elements towards the center of the defect in Group III than in Groups I or II. Group IV defects showed minimal evidence of new bone formation, the defect being filled with fibrous connective tissue and muscle bellies extending from adjacent soft tissues (G, H). nb=new bone; hb=host bone. Scale bar 500 μm (A, C, E, G) and 100 μm (B, D, F, H).

quantitatively similar in Groups I through III at POW 8 and significantly ($p<0.05$) greater than the measured BV in the unfilled Group IV defects (Fig. 3B; Table 2).

Biomechanical testing data

The defects of Groups I–III were mechanically characterized following sacrifice (Fig. 4; Table 2). No significant differences between treatment groups were noted although the mean maximal load and the mean maximal torque were consistently greater in Group I operated femora than in Groups II or III.

Histology

Histological analyses at POW 8 revealed moderately good integration of the parent diaphyseal cortices with new bone in Groups I (Figs. 5A, B) and III (Figs. 5E, F). In both groups the defects were characterized by the presence of a continuum of woven and lamellar bone surrounding islands of silk matrix more centrally with elements of cortical bone more peripherally. Subjectively, the extent of trabecular bone in Group I defects (Figs. 5A, B) was moderately less than that noted in Group III (Figs. 5E, F) defects. Group II defects revealed comparatively less new bone formation than both Groups I and III and that present was principally found adjacent to the parent bone margins (Figs. 5C, D). The Group II silk matrix was often diffusely enveloped by poorly differentiated loose fibrous connective tissue (Figs. 5C, D). While few in number, there were moderately more cartilage elements towards the center of the defect in Group III than in Groups I or II. In Groups I and III, variable staining for bone sialoprotein (BSP) and collagen type I was found in the newly formed matrix at sites of active bone formation. Staining for BSP and collagen type I was less prominent (data not shown). Group IV defects showed minimal evidence of new bone formation, the defect being filled with fibrous connective tissue and muscle bellies extending from adjacent soft tissues (Figs. 5G, H). These tissues did not stain positively for BSP or type I collagen (data not shown).

Discussion

The goal of this study was to assess the ability of rhBMP-2 to augment the osteogenic response to a novel silk fibroin-derived biomaterial when implanted alone or in combination with HMSC populations in a critical size rat femoral defect. Using several analytical tools, we demonstrated prominent bone formation and defect healing in rats implanted with silk scaffolds loaded with rhBMP-2 only (Group III; rhBMP-2/SS), rhBMP-2 and undifferentiated HMSCs (Group II; udHMSC/rhBMP-2/SS), or HMSCs which had been exposed to rhBMP-2 and then expanded in an osteogenic culture medium for 4 weeks prior to implantation (Group I; pdHMSC/rhBMP-2/SS). In comparison, defects which were left unfilled (Group IV) exhibited minimal bone healing.

The impetus for this study was a prior investigation in which we used the same animal model and investigative techniques to assess bone formation following implantation of silk scaffold alone (SS), SS seeded with undifferentiated HMSCs (udHMSC/SS), or SS seeded with pre-differentiated HMSCs (pdHMSC/SS) [10]. While substantial new bone growth along with defect healing was prompted in that study by pdHMSC/SS, implantation of udHMSC/SS or SS alone yielded comparatively less bone regeneration [10]. These data implied the clinical potential of SS as an osteoconductive biomaterial for pdHMSC populations, but an additional impetus was apparently required if optimal bone formation was to occur when SS was implanted alone or with more naive udMHSC populations.

Since another previously published study had demonstrated that the peri-operative addition of a supraphysiological dose of rhBMP-2 to SS or udHMSC/SS could prompt boney healing of a murine critical size cranial defect [11], it was appropriate to repeat the study here using the rat femoral defect model. The latter exposes the implant to an environment which differs from the cranial defect in several respects including the nature of the biomechanical load, the type and extent of enveloping soft tissues, the propensity of the defect to heal [13] and, quite possibly, local influences associated with the fact that, developmentally, long bone formation is endochondral while cranial bone formation is intramembranous.

The potential benefits of peri-operatively combining rhBMP-2 with SS alone or in combination with HMSCs might be several fold. The healing response already demonstrated using pdHMSC/SS could be enhanced. Alternatively, if defect healing could be achieved by peri-operatively adding rhBMP-2 to udHMSC/SS, the laborious (4 weeks) and expensive ex vivo pre-differentiation of the HMSCs along an osteogenic lineage could be avoided. Finally, if satisfactory healing could be achieved using peri-operative rhBMP-2 and SS alone, it might be possible to augment bone healing in acute injuries without waiting to generate ex vivo a responsive stem cell population.

Recombinant human BMP-2 has been well documented as a potent osteoinductive cytokine in a wide range of species including non-human primates and man [3]. Although the recombinant protein was first developed in the late 1980s, it was not until 2001 that it received regulatory approval for clinical use and then only as a bone augmentation agent for a select group of long bone fractures and spinal fusions. Much of this delay can be attributed to the difficulty in identifying an optimal matrix for the protein's local delivery [3]. Presently, a Type I bovine-derived absorbable collagen sponge (ACS) is used clinically but it has drawbacks, for example, minimal load-bearing capacity, sub-optimal handling characteristics on wetting and rhBMP-2 retention that is easily influenced by small differences in pH, anion concentration, cross-linking and ACS mass [16]. Using silk fibroin as a biomaterial offers several advantages over ACS including its more substantial mechanical strength [10], the ability to produce it in a variety of physical formats (e.g., electrospun nets, gels, films and three-dimensional scaffolds) which help facilitate in vivo use [10], and a biodegradability that can be readily manipulated. Additionally, it is readily biocompatible and it has a low inflammatory response once rendered devoid of immunogenic and glycosylated proteins [10]. Finally, there are no known bioburdens associated with this protein-based biomaterial and there is a

long history of human in vivo use of the same protein in suture format.

Our DEXA and radiographic data indicated that the bone mineral content (BMC) of Groups I–III defects was equivalent and significantly greater than the BMC of unimplanted Group IV rats (Table 2). This finding was complemented by our tomographic data which identified a similar pattern (Table 2). However, a comparison of our tomographic data with that generated in a prior study [10] revealed that the peri-operative addition of rhBMP-2 to pdHMSC/SS (Group I) failed to increase the mean BV to the level previously achieved following pdHMSC/SS implantation alone (Table 2) [10]. Similarly, our mechanical testing data show that the Group I implants in this study failed to achieve the mean maximal load and mean maximal torque previously demonstrated in defects treated with pdHMSC/SS [10]. This apparent inability of rhBMP-2 to significantly enhance the osteogenic response to implantation of pdHMSC/SS might reflect the inherent variability of data generated from small sample sizes when using otherwise standardized tomographic and mechanical tests. Alternatively it could be explained by the different preparation of the implants used in this study and that previously reported [10]. In the study reported here the Group I pre-differentiated HMSCs (pdHMSC) evolved in response to a single 2.5 μg application of rhBMP-2 which was adsorped onto the silk scaffolds 1 day prior to cell seeding. The composite implants (HMSCs, rhBMP-2 and silk scaffolds) were then incubated for 4 weeks in spinner flasks prior to implantation in the bone defects. During that time, no additional BMP-2 was supplied. Conversely, the HMSCs seeded on the silk scaffold in the earlier study [10] were exposed to a comparatively greater quantity of rhBMP-2 in the expansion media (250 μg viz 2.5 μg). Furthermore, in that study 250 μg of fresh BMP-2 was supplied twice per week with every medium change [10], while only the media but not the rhBMP-2 were refreshed in the study reported here. Consequently, we might expect that the HMSCs' total exposure to rhBMP-2 during the differentiation and cell expansion process would be greater in the earlier study [10] and hence the cells would be more differentiated towards an osteoblastic phenotype capable of optimally generating bone before their implantation in vivo.

Our data confirm that rhBMP-2 can be combined with SS to singularly prompt neo-osteogenesis and, in this model, moderate defect healing. Under these circumstances the SS was an effective osteoconductive matrix, enabling rhBMP-2's potent osteoinductive up-regulation of the local pluripotent, osteoprogenitor and osteoblastic cell populations. The fact that peri-operative addition of rhBMP-2 to silk scaffold (Group III) prompted consistently more bone formation than that previously generated following implantation of SS only [10] implies the successful and effective SS-mediated delivery of rhBMP-2 to the defect site in this study. While the mean maximal load and mean maximal torque of the resultant bone at POW 8 were less than that generated using pdHMSC/rhBMP-2/SS implants, the data imply some basis for using rhBMP-2/SS implants in acutely injured patients who would be adversely affected by delaying surgery while a responsive cell population was generated. Furthermore, since there was no significant difference between Groups II and III data in this study, there is apparently no basis for supplementing rhBMP-2/SS implants with udHMSCs, effectively avoiding the potential risks associated with the ex vivo culture of HMSCs. It should be noted, however, that when silk scaffold was seeded with udHMSCs in the absence of rhBMP-2, the resultant biomechanical properties of the newly formed bone were significantly greater than those achieved with the implantation of silk scaffold alone [10]. Together these data imply that while udHMSCs and rhBMP-2 can both singularly augment osteogenesis in response to implantation of a silk scaffold biomatrix (i.e. udHMSC/SS or rhBMP-2/SS), their effects are not summative when implanted together (i.e. udHMSC/rhBMP-2/SS). One caveat here is that the implanted MSCs, being of human origin, were xenogeneic and hence quite possibly not optimally matched to the environment. Had autogenous or even allogeneic MSCs been used, it remains possible that greater synergy might have been observed.

The authors recognize several improvements in study design that would have enhanced data generation and interpretation. While the small group sample sizes were adequate for radiographic, densitometric, and tomographic analyses, the inherent variability of data generated using biomechanical tests ideally requires substantially greater specimen numbers for definitive statistical analyses. Similarly, the power of this study could have been enhanced by random selection of the operated limb (left or right rather than all right as was used here) and by using the unoperated contralateral limb as a within-animal control. Additionally, inclusion of a second pdHMSC/rhBMP-2/SS group, in which the HMSCs were exposed to the much larger quantities of rhBMP-2 that were used by Meinel et al. [10], would have offered greater opportunity for commenting on the effect of rhBMP-2 dose on HMSC differentiation. Furthermore, this study did not employ any cell labeling techniques that would have allowed us to confirm that neo-osteogenesis was derived from the recruitment of the implanted HMSCs rather than or as well as from endogenous rat MSCs which migrated to the defect site in response to the rhBMP-2. Lastly, this animal model in which the bone defect is surrounded by large and well vascularized muscle bellies which likely host a generous population of endogenous osteoprogenitor cells may not effectively reveal to us the true benefit of seeding silk scaffold with exogenous osteoprogenitor cells. Future studies might be better off using a more distal location where overlying soft tissues and, presumably, a respondent cell population are less available.

In summary, the data support the use of rhBMP-2 in this rodent long bone defect model for the purposes of augmenting the osteogenic response to silk scaffolds implanted alone or in combination with responsive stem cell populations. Additional studies using larger animal species (e.g., dogs, sheep or goats) which will represent a more clinically pertinent challenge for the implants are now warranted.

Acknowledgments

We thank the NIH Tissue Engineering Resource Center (DK) and the NSF (DK, LM) for support of this research.

References

[1] Deutsche Bank Alex. Brown report; 2001.

[2] Kirker-Head CA. Potential applications and delivery strategies for bone morphogenetic proteins. Adv Drug Deliv Rev 2000;43:65–92.

[3] Kirker-Head CA. Development and application of bone morphogenetic proteins for the enhancement of bone healing. J Orthop Trauma 2005;6:1–9.

[4] Southwood LL, Frisbie DD, Kawcak CE, McIlwraith CW. Delivery of growth factors using gene therapy to enhance bone healing. Vet Surg 2004;33:565–78.

[5] Kraus KH, Kirker-Head C. Mesenchymal stem cells and bone regeneration. Vet Surg 2006;35:232–42.

[6] Altman GH, Diaz F, Jakuba C, Calabro T, Horan RL, Chen J, Lu H, Richmond J, Kaplan DL. Silk-based biomaterials. Biomaterials 2003;24:401–16.

[7] Meinel L, Fajardo R, Hofmann S, Langer R, Chen J, Snyder B, Vunjak-Novakovic G, Kaplan DL. Silk implants for the healing of critical size bone defects. Bone 2005;37:688–98.

[8] Meinel L, Karageorgiou V, Hofmann S, Fajardo R, Snyder B, Li C, Zichner L, Langer R, Vunjak-Novakovic G, Kaplan DL. Engineering bone-like tissue in vitro using human bone marrow stem cells and silk scaffolds. J Biomed Mater Res A 2004;71:25–34.

[9] Asakura T, Kaplan DL. Silk production and processing. In: Arutzen CJ, editor. Encyclopedia of agriculture science. New York, vol. 4; 1994. p. 1–11.

[10] Meinel L, Betz O, Fajardo R, Hofmann S, Nazarian A, Hilbe M, McCool J, Langer R, Vunjak-Novakovic G, Merkle HP, Rechenberg B, Kaplan DL, Kirker-Head C. Silk based biomaterials to heal critical sized femur defects. Bone 2006;39:922–31.

[11] Karageorgiou V, Tomkins M, Fajardo R, Meinel L, Snyder B, Wade K, Chen J, Vunjak-Novakovic G, Kaplan DL. Porous silk fibroin 3-D scaffolds for delivery of bone morphogenetic protein-2 in vitro and in vivo. J Biomed Mater Res A 2006;78:324–34.

[12] Meinel L, Karageorgiou V, Fajardo R, Snyder B, Shinde-Patil V, Zichner L, Kaplan D, Langer R, Vunjak-Novakovic G. Bone tissue engineering using human mesenchymal stem cells: effects of scaffold material and medium flow. Ann Biomed Eng 2004;32:112–22.

[13] Einhorn TA, Lane JM, Burstein AH, Kopman CR, Vigorita VJ. The healing of segmental bone defects induced by demineralized bone matrix. A radiographic and biomechanical study. J Bone Joint Surg Am 1984;66:274–9.

[14] Kraus KH, Kadiyala S, Wotton H, Kurth A, Shea M, Hannan M, Hayes WC, Kirker-Head CA, Bruder S. Critically sized osteo-periosteal femoral defects: a dog model. J Invest Surg 1999;12:115–24.

[15] Sofia S, McCarthy MB, Gronowicz G, Kaplan DL. Functionalized silk-based biomaterials for bone formation. J Biomed Mater Res 2001;54:139–48.

[16] Friess W, Uludag H, Foskett S, Biron R, Sargeant C. Characterization of absorbable collagen sponges as recombinant human bone morphogenetic protein-2 carriers. Int J Pharm 1999;185:51–60.